A Study of Curved Crack Paths in Cold-Formed Corners of High Strength Structural Steel

S. Heinilä, G. Marquis, T. Björk and J. Lepistö

Lappeenranta University of Technology, Department of Mechanical Engineering P.O. Box 20, FI-53851 LAPPEENRANTA, FINLAND; E-mail: sami.heinila@lut.fi

ABSTRACT. *Fatigue crack propagation in cold-formed corners of high-strength structural steel plate-type structures has been investigated. Large- and small-scale test specimens having complex residual stress states and subject to multi-axial cyclic loading have been investigated using both laboratory tests and numerical simulations. Straight, zig-zag and "S" shaped cracks were observed depending on the material strength, range of cyclic loading, residual stress field and multi-axiality of the applied loading. Numerical simulations of residual stresses and linear elastic fracture mechanics were used to help understand the alternate crack paths.*

INTRODUCTION

Cold-forming is a widely used fabrication process for plate welded structures. Cold-formed rectangular hollow section (CFRHS) tubes are frequently fabricated in a two-phase process in which a flat plate is initially cold-formed into a circular mother tube and is then further cold-rolled into its final rectangular shape. The cold-forming process, however, is known to introduce high levels of residual stress which may be either beneficial of detrimental with respect to fatigue strength of the structure. During plate bending or fabrication of a CFRHS, the concave inside corner surfaces experience significant compressive plastic strains. The resulting tensile residual stresses in the bend region enhance the crack propagation during cyclic loading. The bend process also coarsens the initially smooth surface and enhances both micro-cracking and fatigue crack development on the surface [1].

If the residual stresses in a fabricated component are sufficiently high, a crack can propagate even if the applied local stresses are cyclically compressive. Greasly et al. [2] showed that a mode I fatigue crack within a tensile welding residual stress field can grow even when the cyclic external stresses are compressive. However, in this study the cracks arrested after a period of propagation. Hermann [3] tested compact tension aluminium alloy specimens that were pre-compressed in order to create a tensile residual stress field ahead of the notch tip. It was shown that the crack length at which a crack arrested increased with increasing levels of the pre-compression, i.e. an increasing large tensile residual stress field.

In this current study, multi-axial compressive loading was applied to the cold-formed corners of both CFRHS tubes and simple bent plates. Cracks did not arrest, but the crack mode and crack paths were altered. Several distinct crack paths were observed depending on the type and range of cyclic loading, material and residual stress conditions of the specimens. In the case of applied mixed-mode loading, it has been previously reported that the crack growth rate alone is not sufficient for assessing the fatigue strength of a technical structure, but that the strength also depends on the growth direction of the fatigue crack [4,5]. In this study the residual stress field induced a complex multiaxial stress field that had significant influence on the crack growth direction and thus on the lifetime of the structure.

BACKGROUND

The current study was partially motivated by an observed in-service failure of a structure fabricated from of a CFRHS tube made of high-strength steel [1]. The observed crack was long (in the longitudinal direction of the tube) and had a small aspect ratio. It propagated undetected from the inside corner through the tube wall. The resulting fatigue crack had an "S" shaped path as seen in Fig. 1.

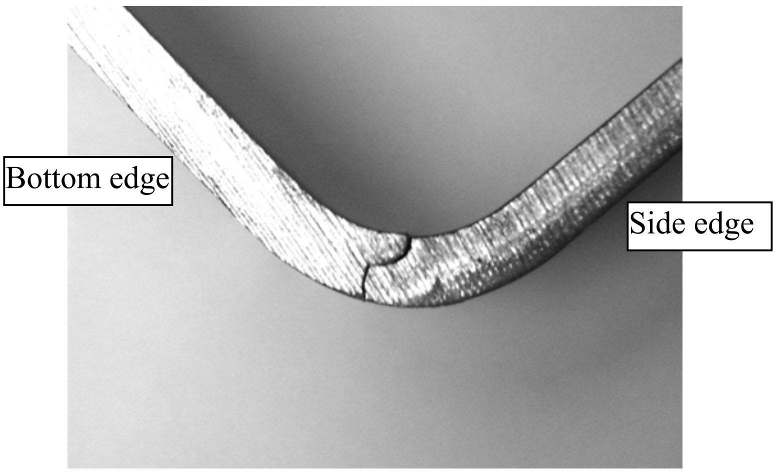

Figure 1. Observed crack path from a tube that failed in service.

LABORATORY TESTS

Analytical and experimental studies were planned to both reproduce the observed cracking behaviour and to better understand the fatigue crack propagation behaviour. Both large and small scale specimens were tested.

Large Scale Specimens

The large scale laboratory specimen was a CFRHS manufactured by cold rolling and was identical to that used in the failed in-service structure. The test configuration included two beam-type specimens of which four corners, two of each specimen, were monitored for cracks using back side strain gauges, i.e. strain gages were glued to the outside corner of the tube. The CFRHS profile is generally shown in Fig. 2 and a schematic of the test arrangement is shown in Fig. 3. In total, eight specimens were tested. The CFRHS was fabricated from high strength steel with nominal yield stress f_y = 650 MPa. The middle support shown in Fig. 3 consisted of a series of rollers that travelled back and forth in-phase with the applied bending loading. The lateral roller translation was about 10% of the length of the beam-type specimen. Fatigue cracking was observed within this region of travel and also in the regions just beyond travel of the rollers. Multiple cracks initiated near the centre of the inner corner of the tube as can be seen in Fig. 4.

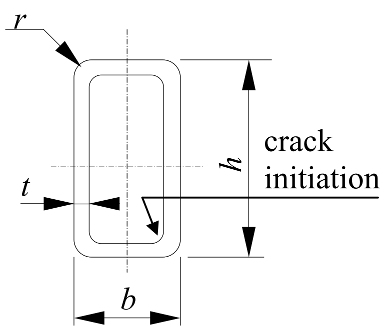

Figure 2. CFRHS profile.

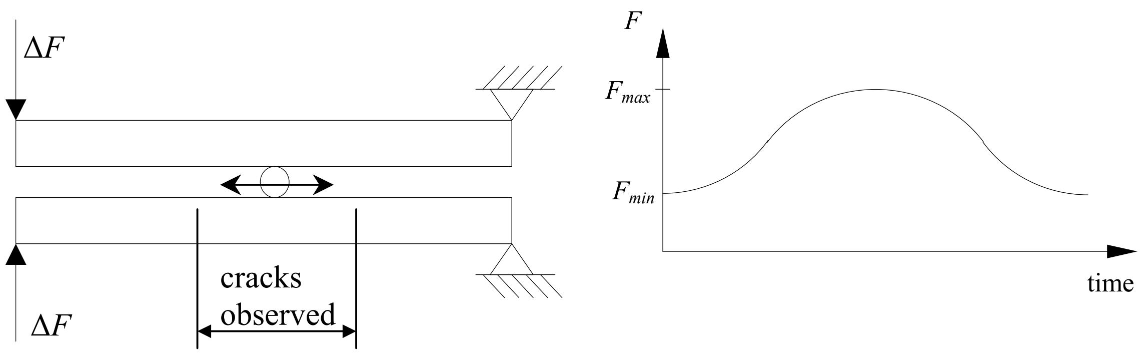

Figure 3. Testing configuration and schematic diagram showing the applied loading ΔF.

Figure 4. Cracks initiated along the inner corner of the tube. Dark regions are cracks highlighted using a dye-penetrant solution.

The residual stresses at the centre of the corner were measured using the X-ray diffraction method. Residual stresses on the inner and outer surfaces and at small depths from the inner surface were measured. Measured tensile residual stresses on the inner surface were in the range 30…50% of the nominal yield strength of the material. Results for one tube corner are shown in Table 1. Depth measurements in Table 1 are presented as a portion of the wall thickness, *t*, of the tube. The outer surfaces of the tubes were found to have compressive residual stresses.

Table 1. The tangential residual stresses σ_{res} at the centre of the CFRHS corner

depth	$\boldsymbol{\sigma_{res}}$	
	MPa	**± MPa**
0 (inner surface)	213	25
0.003 * *t*	313	32
0.006 * *t*	292	17
0.012 * *t*	252	33
0.022 * *t*	188	33
0.035 * *t*	174	33
0.051 * *t*	173	44
0.066 * *t*	124	55
1.000 * *t* (outer surface)	-73	44

Residual stresses along the inner corner at positions other than the centre were also measured. These stresses were also tensile, but the magnitudes were lower and are not here reported. Crack initiation was observed to occur in the centre of the corner where the tensile residual stress was highest. Numerous small cracks, longitudinal with respect to the beam-type specimen, propagated along the inner surface and eventually joined to form a single long small aspect ratio crack. This crack then propagated transverse through the wall of the tube. Crack growth was initially orthogonal to the inner surface of the tube. However, near the neutral plane of the wall, the crack appeared to turn 90°

with respect to the original direction forming a zigzag crack as seen in Fig. 5. Closer inspection revealed, however, that the crack did not turn but rather joined with other cracks that had initiated tangential to the tube corner radius near the centre of the wall. This is seen in Fig. 6.

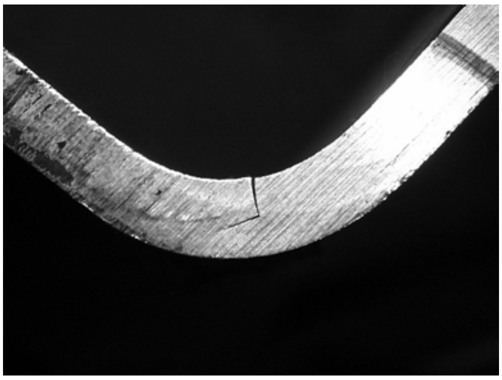

Figure 5. Crack kinking found in large scale laboratory specimen.

Testing also included two beam-type specimens that were thermal treated so as to relieve, or at least reduce, the residual stresses in the beam corners. These specimens showed completely different cracking behaviour. No cracks were observed to initiate on the inner surfaces of these tubes. Cracks in these specimens initiated on the outer surface of the tube due to contact fatigue with the moving middle support rollers. Fatigue strength was significantly improved with respect to the non-heat treated beams. This observation clearly demonstrated that the residual stresses have a major effect on fatigue crack path and fatigue strength of the structure.

Small Scale Specimens

Three alternate small scale specimen geometries were tested. In some cases alternate material strengths were also investigated. The small scale specimens allowed alternate load modes to be applied to the corner regions.

CFRHS specimens

Sections of CFRHS tubes were fatigue tested using external compressive loading as shown in Fig. 7. These small scale CFRHS specimens were made of structural steel with yield strength f_y = 650 MPa. Loading was applied to opposite corners so as to create pure bending condition in the corners. Some specimens were found to fail from the corners under applied cyclic compressive stresses while other specimens fractured in the corners subject to applied cyclic tension. In all these cases the cracks propagated relatively straight through the wall thickness as seen in Fig. 7. Similar crack path have previously been reported by Bäckström et al. [6].

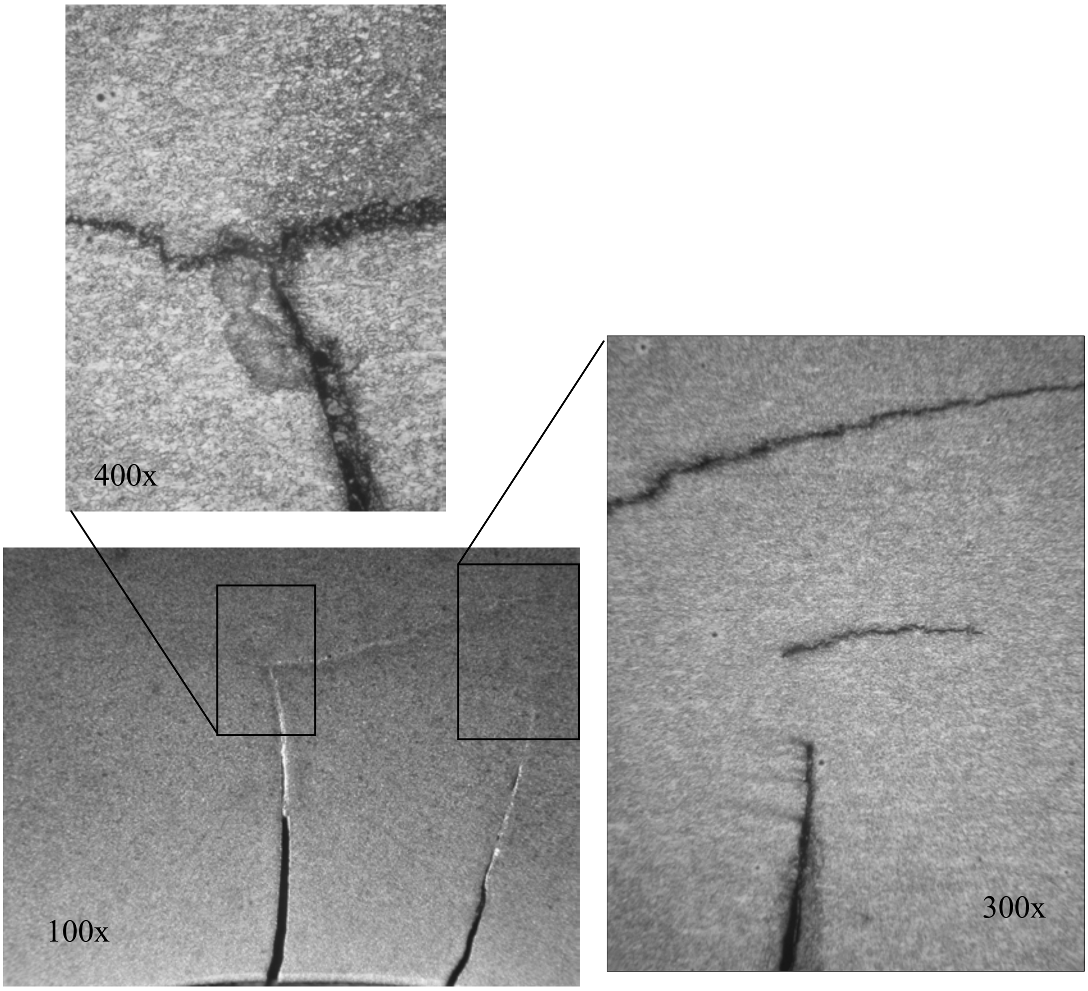

Figure 6. Crack kinking found in large scale laboratory specimen turned out to be a new crack initiation.

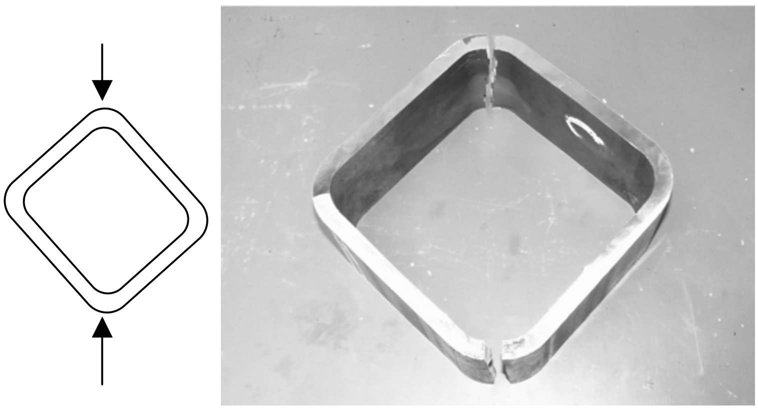

Figure 7. Straight crack paths were found in a small scale specimen cut from CFHS tubes subject to compressive external loading.

"L" specimens

Small scale "L" shaped plate specimens were manufactured both by cold forming small plate sections and by cutting corner sections from CFRHS tubes. These were fatigue tested using compressive loading as shown in Fig. 8. In the case of specimens produced by plate bending, the initially straight plates were bent in a single operation with special tools to achieve a final angle of 90° angle with a defined inner radius, *r*. The radius and the material were chosen so as to be similar to the large beam-type specimens.

During testing, the specimens were clamped along one end and an external cyclic force, ΔF was applied at the start position of the corner, see Fig. 8. This loading mode induced a bending stress in the corner region similar to that produced by the compression loading shown in Fig.7. However, the test configuration in Fig. 8 also produced a significant alternating shear stress component. The local stress state in the corner region was, therefore, similar to the stress state in the large beam-type specimens.

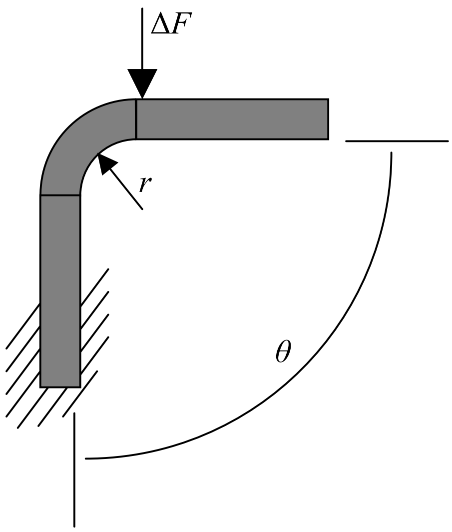

Figure 8. Loading configuration for small scale "L" plate specimens.

Fatigue cracking was always observed to initiate on the inside surface of the corner. Curvilinear crack paths similar to the service failure crack (see Fig. 1) were observed in specimens cut from CFRHS tubes. Specimens formed by simple bending of plates with nominal yield strengths greater than 650 MPa had straight crack paths. Typical paths are seen in Fig. 9.

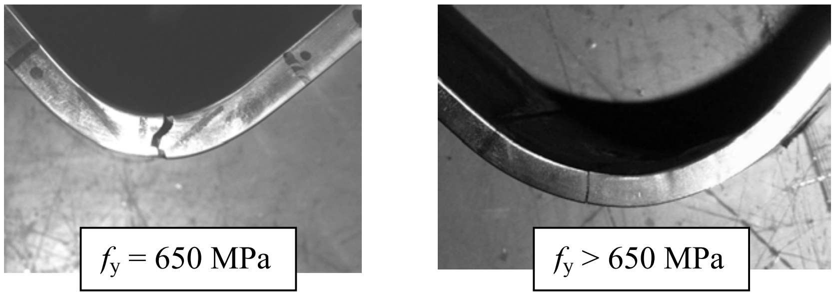

Figure 9. Samples of curvilinear and straight crack paths observed in small scale “L” plate specimens.

NUMERICAL MODELLING

In order to better understand the initial residual stress state, the finite element method was used to simulate the cold forming operation for a structural tube [7]. The computed through-thickness distribution of tangential residual stresses is shown in Fig. 10. Numerous simplifying assumptions were made in this simulation and, as a result, the computed residual stresses were not in full agreement with the stresses measured by X-ray diffraction. The errors were mainly due to the overly simple material model implemented and the use of a 2D simulation. The true cold forming process for a CFRHS tube is 3D and difficult to simplify.

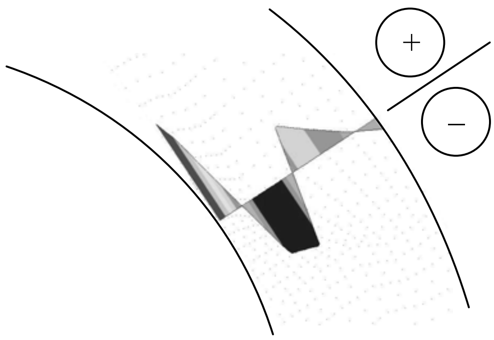

Figure 10. Tangential residual stresses of CFRHS according to FE-simulation.

Residual stresses along two crack paths were assessed. Paths were chosen based on the observed crack paths in the laboratory test specimens and the in-service failure. The first path was “S” shaped (see Fig. 1) while the second was straight through the thickness in the corner region (see Fig. 7). The stress intensity factors (SIF’s), K_I and K_{II}, as a function of crack length due to the residual stress alone were calculated. These are shown in Fig. 11. For calculations residual stress distribution with crack growth was assumed, however, contact between the crack faces was not included so SIF values contain some errors, especially in the cases where $K_I < 0$. Some mesh simplifications were also used. K_I and K_{II} could be calculated based on the J-integral or its domain integral conversion [8]. For Fig. 11 it is clearly seen that K_I for the straight crack approaches zero at a crack depth of about 3 mm. On the other hand, K_I remains greater than zero in the case of a curvilinear crack path. If the external cyclic loading also produces compressive stresses, it is clear that a straight crack path through the thickness is not physically possible. On the other hand, the curvilinear crack will remain open even at greater crack depths. The fact that the mode II SIF becomes negative is not significant.

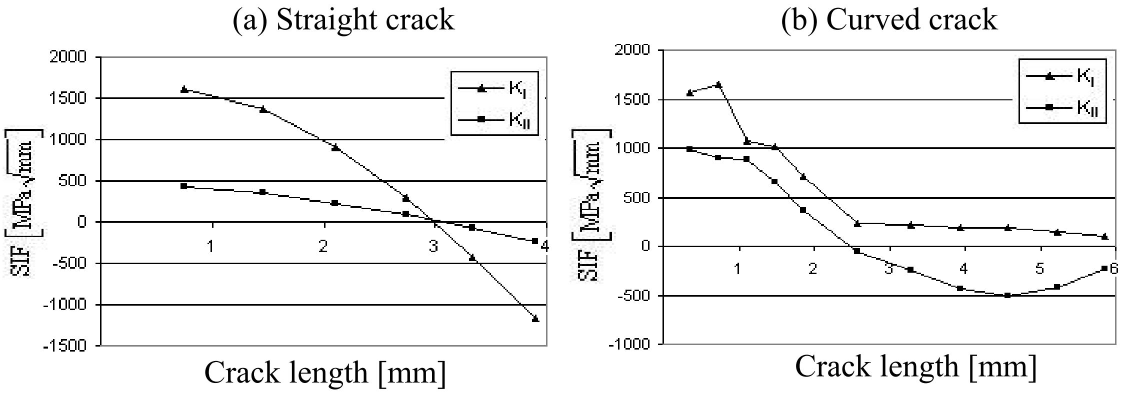

Figure 11. Stress intensity factors for straight (a) and curved crack (b) in case of no external loading.

Estimates of the residual tangential stress redistribution due to crack advance were also obtained for the two crack paths. The residual stress field for the “S” shaped crack case evolves into a simple tension-compression field as the crack approaches the neutral plane, see Fig. 12. In the case of a straight crack, the tensile residual stresses ahead of crack tip slowly diminish and compressive stresses are developed, see Fig. 13.

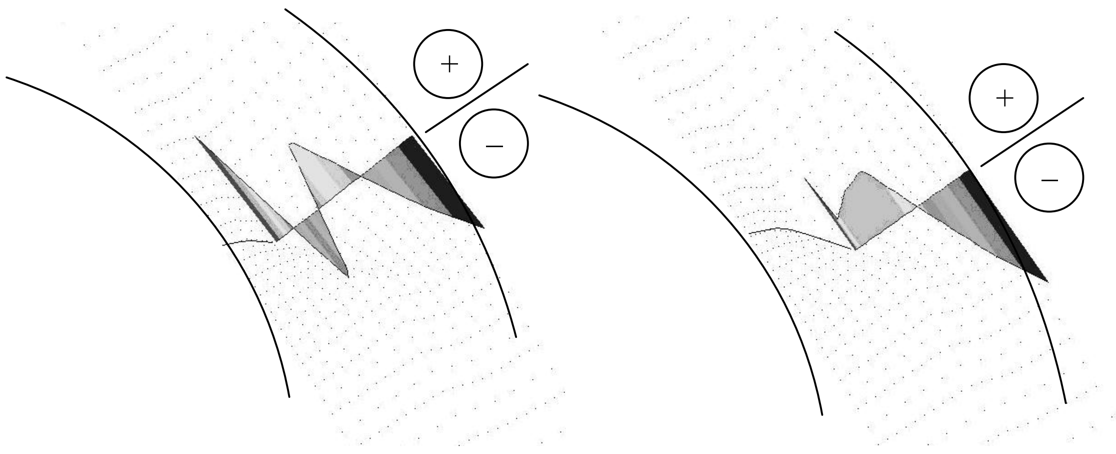

Figure 12. Estimated redistributed residual stresses tangent to the corner in the case of a curved crack.

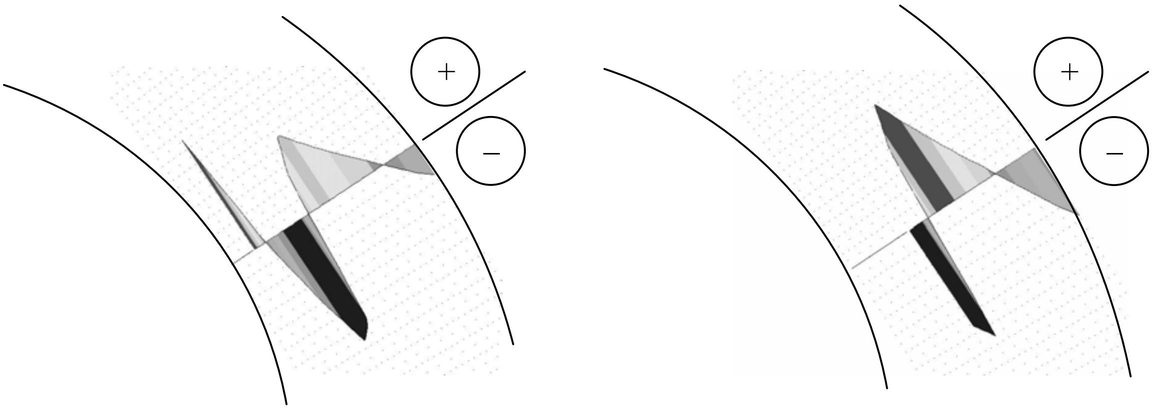

Figure 13. Estimated redistributed residual stresses tangent to the corner in the case of a straight crack.

DISCUSSION

The local tangential stress on inside surface at the corner is the sum of the stress induced by the external loading and tensile residual stress. In general the local tangential stress under alternating external loading can be stated as

$$\sigma^{\theta}_{\min} = \sigma^{\theta\mathrm{res}} + \sigma^{\theta\mathrm{ext}}_{\min} \qquad (1\ a)$$

$$\sigma^{\theta}_{\max} = \sigma^{\theta\mathrm{res}} + \sigma^{\theta\mathrm{ext}}_{\max} \qquad (1\ b)$$

$$\Delta\sigma^{\theta} = \sigma^{\theta}_{\max} - \sigma^{\theta}_{\min} \qquad (2)$$

where $\sigma^{\theta\mathrm{res}}$ is local tangential residual stress, $\sigma^{\theta\mathrm{ext}}$ is local tangential stress caused by remote external loading and $\Delta\sigma^{\theta}$ is the range of the local tangential stress caused by the external loading cycle. The range of local stress is clearly independent of the residual stress while the mean stress depends on both the residual stress and the applied external stress.

Tensile or compressive mean stresses are known to have a strong influence on whether a crack grows predominantly by mode I or mode II [9,10]. Once a crack begins to branch, the mean stress does not influence the orientation of the brack crack. Branch cracks initially propagate in the direction perpendicular to the local maximum tangential stress ($\sigma^{\theta}_{\max}$) and gradually changes to the direction perpendicular to the remote principal stresses [11,12]. Residual stresses would therefore be expected to have an influence on the dominant mode of crack growth but do not promote growth in arbitrary direction. The issue of residual stresses is of course further complicated by the fact that they are secondary stresses that continuously redistribute with crack advance so as to be self-equilibrating. Residual stresses also frequently have large grandients that change from tensile to compressive over very short distances.

As mentioned previously, the loading configuration illustrated by Fig. 8 produces both tangential stresses and shear stresses in the corner region. A fatigue crack that initiates on the inner surface of the corner will initially propagate in the direction perpendicular to the local maximum tangential stress range. Even though the external load produces a local stress that alters between zero and a compressive minimum, the crack will be open during the cycle due to the high tensile residual stresses. Eventually the mode I crack growth rate will reduce or go to zero as the crack proceeds into the region of reduced tensile residual tangential stresses or even into the region of compressive residual stress. The driving force for a straight crack is very small due to the significant compressive residual tangential stresses associated with this path, see Fig. 13. If the alternating shear stress was sufficiently small, the crack would arrest as was observed in the previously referenced cases [2, 3].

With relatively small external loads, the crack advance is small and the crack path turns. The turning is aided by the redistribution of the residual stresses in which the stresses tangential to the crack tip plane remain tensile. The alternating shear stresses near the neutral plane of the plate combined with a small tensile K_I are sufficient to continue crack advance on the curved path. The propagation progresses in this fashion until the crack reaches the neutral plane and the crack has turned to direction of the maximum shear stress. After a short period of crack extension along the centre of the plate, mode I crack growth caused by the external loading is again preferable and a branch crack develops that rapidly advances through the plate thickness. This process produces the “S” shaped crack path as seen in Fig. 1.

The zigzag crack path seen in Fig 5 for the large laboratory specimen was subject to loading similar to the in service beam shown in Fig 1. The in-service beam had an “S” shaped crack. The only significant difference is the amplitude of applied loading which is greater in the case of the zigzag crack. The large stress amplitude leads to the network of tensile and shear cracks observed in Fig. 6. In this case the main crack does not turn as in the case of a single crack, but the straight mode I crack links to a mode II crack initiated near the neutral axis of the plate. The final branch crack that leads to failure is the same for both the “S” crack and the zigzag crack. The increased stress amplitude probably also has some influence on the residual stress redistribution, e.g., Lee et al. [13] found that residual stress redistribution was affected also by the cyclic loading range. This issue, however, is not fully understood for the cold-formed corners studied here and remains an area for further investigation.

An interesting contrast exists for the small “L” shaped specimens cut from CFRHS tubes and those formed by bending of simple plates. An “S” shaped crack, similar to that found in the failed-in-service beam, was observed for specimens cut from tubes sections while straight cracks occurred for plate bending specimens (Fig. 9). The external loading conditions were identical and the major difference was the residual stress state. The plate bend specimens had somewhat higher yield strength and therefore potentially higher residual stresses. However, the corner radii and plate thickness were slightly different. Residual stress measurements for the simple bending case have also not yet been done and this difference in behaviour is not yet fully explainable.

The loading configuration shown in Fig. 7 produces predominantly tangential normal stresses and only negligible shear stresses. The resulting crack paths observed for the small scale CFRHS specimens were nearly straight (Fig. 7). In this case mode I crack initiation is assisted by the tensile residual stresses. The combination of external loading and redistributing residual stresses does not lead to a crack arrest condition.

CONCLUSIONS

Fatigue crack propagation in cold-formed corners of high-strength structural steel plates has been investigated using large- and small-scale laboratory specimens, finite element analysis and linear elastic fracture mechanics. The cold-formed corners have complex residual stress states and were subject to multi-axial cyclic loading. Straight, zig-zag and “S” shaped crack paths were observed. The compressive tangential residual stresses due to cold forming and the alternating shear stresses due to the external loading were found to have a dominating influence of the observed fatigue crack path.

REFERENCES

1. Heinilä, S., Björk, T., Marquis, G., Bäckström, M., Ilvonen, R. (2004) In: *Proceedings of ECF15*, Stockholm.
2. Greasley, A., Naylor, S. G. W. (1986) *Engng Fract. Mech*., **24**, 717-726.
3. Hermann, R. (1994) *Fatigue Fract. Engng Mater. Struct*. 17, 93-103.
4. Sumi, Y. (2003) In: *Proceedings of FCP 2003*, Parma.
5. Filippini, M., Giglio, M., Gorla, C., Rosa, F. (2003) In: *Proceedings of FCP 2003*, Parma.
6. Bäckström, M., Savolainen, M., Ilvonen, R., Laitinen R. (2002) In: *Proceedings of FATIGUE 2002*, Stockholm, 277 – 302 .
7. Heinilä, S., Björk, T., Marquis, G., Ilvonen, R. (2004) In: *Proceedings of ECCOMAS 2004*, Jyväskylä.
8. Lei, Y., O’Dowd, N. P., Webster, G. A. (2000), *Int. J. Fract*., **106**, 195-216.
9. Marquis, G. and Socie, D., (2000) *Fatigue Fract. Engng Mater. Struct*. **23**, 293-300
10. Pook, L. P., (2002) *Crack Paths*, WIT Press, Southhampton.
11. Murakami, Y., Takahashi, K., Toyama, K. (2003) In: *Proceedings of FCP 2003*, Parma.
12. Tanaka, K., Kato, T., Akiniwa, Y. (2003) In: *Proceedings of FCP 2003*, Parma.
13. Lee, Y., Chung, C., Park, Y., Kim, H. (1998) *Int. J. Fat*. **20,** 565-573.